JOURNAL OF GEOPHYSICAL RESEARCH, VOL. 115, D00K13, doi:10.1029/2009JD013145, 2010

Mixing of Asian dust with pollution aerosol and the transformation of aerosol components during the dust storm over China in spring 2007

Kan Huang,[1] Guoshun Zhuang,[1] Juan Li,[1] Qiongzhen Wang,[1] Yele Sun,[2] Yanfen Lin,[1] and Joshua S. Fu[3]

Received 4 September 2009; revised 10 February 2010; accepted 23 February 2010; published 21 July 2010.

[1] An intensive spring aerosol sampling campaign over northwestern and northern China and a megacity in eastern China was conducted in the spring of 2007 to investigate the mixing of Asian dust with pollution aerosol during its long-range transport. On the basis of the results of the three sites near dust source regions (Tazhong, Yulin, and Duolun) and a metropolitan city (Shanghai), three dust sources, i.e., the western high-Ca dust in the Taklimakan Desert, the northwestern high-Ca dust and the northeastern low-Ca dust in Mongolia Gobi, were identified on the basis of the air mass trajectories and the elemental tracer analysis (e.g., Ca/Al, SO_4^{2-}/S, Ca^{2+}/Ca, and Na^+/Na). The western dust was least polluted in comparison to the other two dust sources. The results evidently indicated that the dust could have already mixed with pollution aerosol even in near dust source regions. The concentrations of As, Cd, Cu, Pb, Zn, and S were elevated several times at all sites during dust days, showing the entrainment of pollution elements by dust. The secondary SO_4^{2-} was observed to show much higher concentration due to the heterogeneous reaction on the alkaline dust during dust storm, while the concentrations of NO_3^- and NH_4^+ decreased owing to the dilution of the local pollution by the invaded dust. The western dust contained relatively low anthropogenic aerosols, and it mainly derived from the Taklimakan Desert, a paleomarine source. The northwestern dust had a considerable chemical reactivity and mixing with sulfur precursors emitted from the coal mines on the pathway of the long-range transport of dust. The northeastern dust reached Shanghai with high acidity, and it became the mixed aerosol with the interaction among dust, local pollutants, and sea salts. Comparison of the speciation of the water-soluble ions on both nondust and dust days at all sites illustrated the evolution of major ion species from different dust sources during the long-range transport of dust. The mixing mechanisms of the dust with the pollution aerosol on the local, medium-range, and long-range scale revealed from this study would improve the understanding of the impacts of Asian dust on the regional/global climate change.

Citation: Huang, K., G. Zhuang, J. Li, Q. Wang, Y. Sun, Y. Lin, and J. S. Fu (2010), Mixing of Asian dust with pollution aerosol and the transformation of aerosol components during the dust storm over China in spring 2007, *J. Geophys. Res.*, *115*, D00K13, doi:10.1029/2009JD013145.

1. Introduction

[2] The Asian dust storms originating from arid regions and deserts located in Mongolia and China are natural phenomena. These dust storms impact the air quality of densely populated downstream areas such as China, Korea, and Japan, and they can exert far-reaching influence on the global biogeochemical cycle [*Zhuang et al.*, 1992]. Acidification of mineral dust particles reacted by those acid gases would mobilize the dissolution ratio of iron and affect the rate of carbon fixation in high-nutrient low-chlorophyll regions of the Pacific Ocean [*Meskhidze et al.*, 2003]. The entrained airborne carbonate (as high as 44.8 Tg yr^{-1}) by Asian dust may provide an important atmospheric alkaline carbon reservoir for large-scale climatic and environmental changes by increasing the alkalinity of ocean water in the Pacific Ocean and buffering the atmospheric acidity of east Asia [*Cao et al.*, 2005]. The dust can directly affect the climate by scattering and absorbing the sunlight radiation and indirectly affect

[1]Center for Atmospheric Chemistry Study, Department of Environmental Science and Engineering, Fudan University, Shanghai, China.
[2]Atmospheric Sciences Research Center, State University of New York at Albany, Albany, New York, USA.
[3]Department of Civil and Environmental Engineering, University of Tennessee, Knoxville, Tennessee, USA.

0148-0227/10/2009JD013145

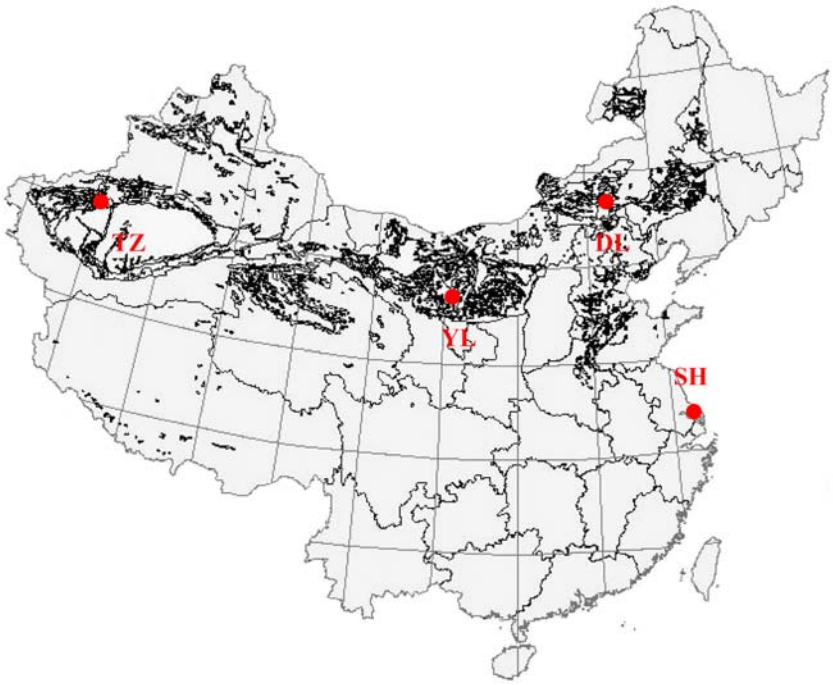

Figure 1. Sampling sites in spring 2007 (TZ, Tazhong; YL, Yulin; DL, Duolun; SH, Shanghai). The deserts are marked by the shadows in the map. (Approximate latitude and longitude of China: 18°15′N to 53°30′N and 74°E to 134°30′°E.)

climate by acting as cloud condensation nuclei as a result of the involvement of dust's chemical reactivity [*Arimoto*, 2001]. The combined anthropogenic forcing of dust, nitrate, and sulfate aerosols is estimated to be a negative radiation forcing of −0.1 W/m^2 [*Bauer et al.*, 2007].

[3] There are two dominant source regions of eolian dust raised from China and its surrounding regions, which are the Taklimakan Desert in western China and the Gobi Desert in Mongolia and northern China [*Sun et al.*, 2001]. Dust aerosols lifted by the strong surface winds can be transported through the atmosphere for thousands of kilometers to Beijing [*Sun et al.*, 2005; *Guo et al.*, 2004], Taiwan [*Lee et al.*, 2006], Japan [*Ma et al.*, 2005; *Fan et al.*, 1996], Korea [*Mori et al.*, 2003; *Kim et al.*, 2004], and even further to the North Pacific [*Matsumoto et al.*, 2004; *Ooki and Uematsu*, 2005] and North America [*Leaitch et al.*, 2009; *Sun et al.*, 2009; *McKendry et al.*, 2008]. It has been found that dust particles were mixed well with sulfate, nitrate [*Sun et al.*, 2005; *Shen et al.*, 2007], sea salt [*Fan et al.*, 1996], pollution elements Se, Ni, Pb, Br, and Cu [*R. Zhang et al.*, 2005], black carbon [*Kim et al.*, 2004], VOCs [*Cheng et al.*, 2006] and polycyclic aromatic hydrocarbons [*Hou et al.*, 2006] during the transport. Numerical models with respect to dust have also been utilized to study interactions of mineral dust and pollutants [*Zhao et al.*, 2007b], sea salt particles, and clouds [*Levin et al.*, 2005]. Besides the mixing processes on the transport pathway of the dust, it is common for dust to be mixed with pollution aerosol even at those places close to the dust source region [*Arimoto et al.*, 2004; *Xu et al.*, 2004]. However, *D. Zhang et al.* [2005] found that Asian dust plume and polluted air masses did not mix with each other and were separated in two consecutive air parcels. Therefore, understanding the various effects of dust on climate and the global biogeochemical cycles requires information on the transport pathways, chemical and physical characteristics of dust, and the transformation of dust components, which evolve and finally change the optical properties of the dust particles. In this paper, a network of four ground sampling sites was established to characterize the chemical properties of Asian dust storms that occurred in 2007, explore the mixing mechanisms of dust with pollution aerosol, and distinguish different dust sources by introducing new elemental tracers. The results would elucidate the importance of the long-range transport of Asian dust for climate change and its implication of the mixing of dust with pollution aerosol during transport.

2. Experiment

2.1. Sampling

[4] A spring sampling campaign of $PM_{2.5}$ and TSP aerosol by manually collecting filters was carried out from 20 March to 20 April 2007. An intensive ground monitoring network, consisting of four sites along the pathway of the dust storm across China, was set up to monitor the dust episodes. The locations of four sites are shown in Figure 1. Tazhong (TZ), which is located in the Taklimakan Desert in Xinjiang Uygur Autonomous Municipality, represents the upstream of the western Asian dust source [*Li et al.*, 2008]. Yulin (YL) is located in the northern ShannXi Province, at the junction of the Gobi desert and the Loess Plateau. Duolun (DL) is located in the middle of the northeastern Inner Mongolia, close to the Hunshandake desert, one of the important dust sources in northern China [*Cheng et al.*, 2005]. Shanghai (SH) is the biggest city in China and it is located in the Yangtze River Delta region on the eastern

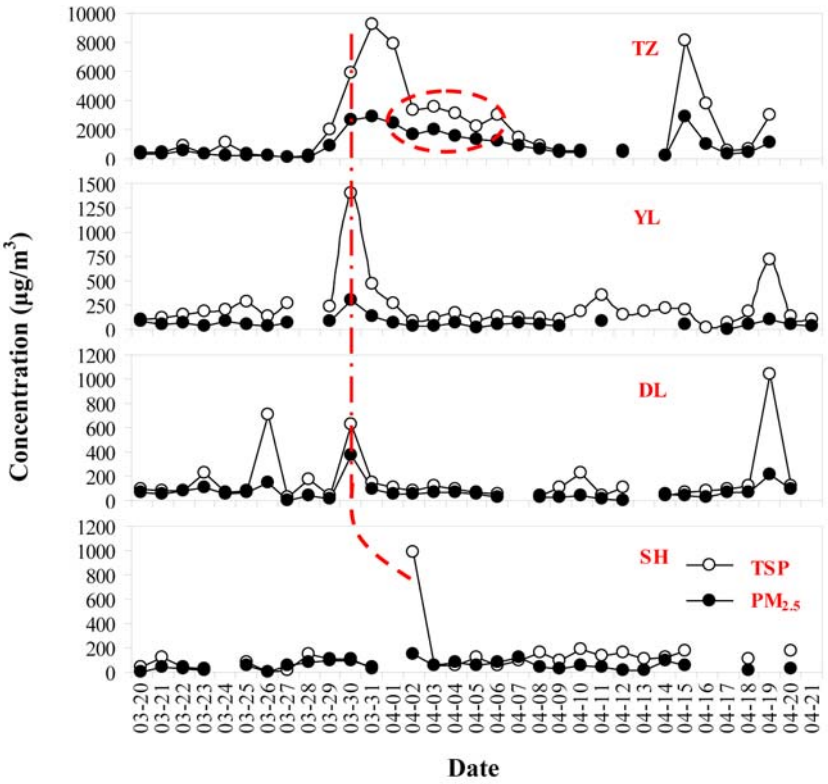

Figure 2. Temporal variations of $PM_{2.5}$ and TSP at four sites (dust episode marked as dash-dotted line).

coast of China. The sampling duration time for each sample was generally 24 h. More samples with shorter time duration were collected during the dust storm days in order to better characterize the transformation and evolution of aerosol components. A total of 264 aerosol samples were collected on Whatman® 41 filters (Whatman Inc., Maidstone, UK) by medium-volume samplers (model: (TSP/PM_{10}/$PM_{2.5}$)-2, flow rate: 77.59 L min^{-1}). All those filters were weighed before and after sampling with an analytical balance (Sartorius BT 25s, reading precision 10 μg) after stabilizing under constant temperature (20 ± 1°C) and relative humidity (40 ± 2%).

2.2. Chemical Analysis

2.2.1. Ion Analysis

[5] One fourth of each sample and blank filter was extracted ultrasonically by 10 mL deionized water (18MΩcm^{-1}). After passing through microporous membranes (pore size, 0.45 μm; diameter, 25 mm), the pH values of filtrates were determined by a pH meter (model: LIDA PHS-2C) with a glass electrode.

[6] Eleven inorganic ions (SO_4^{2-}, NO_3^-, F^-, Cl^-, NO_2^-, PO_4^{3-}, NH_4^+, Na^+, K^+, Ca^{2+}, Mg^{2+}) and five organic acids (formic, acetic, oxalic, malonic acid, and methylsulfonic acid (MSA)) were analyzed by ion chromatography (IC; Dionex ICS 3000, USA) which consists of a separation column (Dionex Ionpac AS 11), a guard column (Dionex Ionpac AG 11), a self-regenerating suppressed conductivity detector (Dionex Ionpac ED50), and a gradient pump (Dionex Ionpac GP50). The detail procedures were given elsewhere [*Yuan et al.*, 2003].

2.2.2. Element Analysis

[7] Half of the sample filters were digested at 170°C for 4 h in high-pressure Teflon digestion vessel with 3 mL concentrated HNO_3, 1 mL concentrated HCl, and 1 mL concentrated HF. After cooling, the solutions were dried, and then diluted to 10 mL with distilled deionized water. A total of 19 elements (Al, Fe, Mn, Mg, Ti, Sc, Na, Sr, Ca, Co, Cr, Ni, Cu, Pb, Zn, Cd, V, S, and As) were determined by inductively coupled plasma atomic emission spectroscopy (ICP-AES; Model: ULTIMA, JOBIN-YVON Company, France). The detailed analytical procedures were given elsewhere [*Zhuang et al.*, 2001; *Sun et al.*, 2004].

2.2.3. Air Mass Trajectory Analysis

[8] Hybrid Single-Particle Lagrangian Integrated Trajectory (HYSPLIT) model from Air Resources Laboratory (ARL) of National Oceanic and Atmospheric Administration (NOAA) was used to compute forward and backward air trajectories at model vertical velocity by using GDAS archived meteorological data set (R. Draxler and G. Rolph, HYSPLIT (HYbrid Single-Particle Lagrangian Integrated Trajectory) Model, 2003, http://www.arl.noaa.gov/ready/hysplit4.html; G. Rolph, Real-time Environmental Applications and Display sYstem (READY), 2003, http://www.arl.noaa.gov/ready/hysplit4.html).

3. Results and Discussion

3.1. General Description of the Dust Episodes

[9] The temporal variations of the concentrations of $PM_{2.5}$ and TSP at four sampling sites are presented in Figure 2.

Table 1. Average Concentrations of $PM_{2.5}$ and TSP and Ratios of $PM_{2.5}$/TSP and Mineral/TSP in ND and DS at Four Sites[a]

	Site							
	TZ		YL		DL		SH	
	ND	DS	ND	DS	ND	DS	ND	DS
$PM_{2.5}$	198.9	992.3	52.5	300.5	55.8	285.5	49.8	153.1
TSP	472.4	4198.6	167.7	1181.3	98.7	909.4	99.4	806.2
$PM_{2.5}$/TSP	0.42	0.26	0.31	0.25	0.54	0.31	0.50	0.19
Mineral/TSP	0.78	0.75	0.65	0.80	0.54	0.60	0.38	0.66

[a]Concentrations are given in $\mu g/m^3$. ND, nondust; DS, dust storm; TZ, Tazhong; YL, Yulin; DL, Duolun; and SH, Shanghai.

Missing points are due to the maintenance or malfunction of instruments. The dust episodes are highlighted by the dashed lines and circles. An intensive and continual dust event was observed in TZ from 29 March to 7 April. During this period, the average concentration of TSP was 4198.6 $\mu g/m^3$ with the peak value of 9607.44 $\mu g/m^3$ on 31 March. Concurrent dust events were also observed in YL and DL on 30 March with the peak values of 3186.98 and 1381.69 $\mu g/m^3$, respectively. On 2 April, SH encountered the highest-ever-recorded floating dust event with the peak concentration of 1340.41 $\mu g/m^3$. The average concentrations of $PM_{2.5}$ and TSP in nondust periods (ND) and dust storm periods (DS) at four sites are presented in Table 1, following the sequence of TZ > YL > DL > SH. The ratios of $PM_{2.5}$/TSP were also listed in Table 1 to show the size distribution of the dust aerosol at each sampling site. In comparison with the nondust days, the ratios of $PM_{2.5}$/TSP during the dust storm periods had a significant decrease at all sites, indicating the entrainment of coarse particles. The $PM_{2.5}$/TSP ratio of Shanghai dropped drastically to 0.19 during the dust day, the lowest among four sites, which perhaps implied that dust had the most prominent impact on the downstream regions. To quantify the contribution of mineral aerosol to the total aerosol mass, it was calculated by summing the major mineral elements with oxygen for their normal oxides, which was [Mineral concentration] = 2.2[Al] + 2.49[Si] + 1.63[Ca] + 2.42[Fe] + 1.94[Ti] [*Malm et al.*, 1994], where the concentration of Si was estimated using the Si/Al ratio of 2.80 for TZ from the results of the individual particle analysis (J. L. Li, manuscript in preparation, 2010) and 3.43 for the other three sites by using its ratio of crust abundance. The average mass percentages of the mineral aerosol in TSP are shown in Table 1. No distinct differences between ND and DS were found in TZ, YL, and DL. These three sites are located in or close to the origin of the dust source, thus less anthropogenic pollutants are expected. However, the ratios of mineral/TSP were lower than unity, which indicated that even at the source regions of dust, there were still significant contribution of the components from other sources, e.g., organics, and secondary inorganic species (SO_4^{2-}, NO_3^-, NH_4^+) besides the minerals. This indicated that the mineral aerosols have possibly already mixed with pollutants even at the dust source regions. For instance, although YL is located in the northern edge of Loess Plateau, one of the dust sources in China, it is surrounded by some big coal mines, and the usage of coal and coal burning would surely contribute a considerable fraction to the aerosol composition there. The biggest deviation of the mineral/TSP ratio between ND and DS was found in Shanghai, with the ratio of 38% and 66% in ND and DS, respectively. Shanghai is a highly developed city with huge industry and traffic emissions; the anthropogenic sources contributed most in the nondust days, while the mineral dust apparently dominated in the dust days.

3.2. Source Identification

3.2.1. Source Identification by Air Mass Trajectories

[10] The backward trajectory is often applied to characterize the origin of air masses by using the HYSPLIT4 (Hybrid Single-Particle Lagrangian Integrated Trajectory) Model developed by NOAA/Air Resources Laboratory and the results are shown in Figure 3. Clearly, the dust storm, which reached YL on 30 March, originated from Mongolia and then entered the west of the Inner Mongolia and the Loess Plateau in China (Figure 3a). The dust storm in DL occurred in the eastern Mongolia Gobi and transported through the Hunshandake Desert and Horqin Desert (Figure 3b). As for SH, the air masses moved mainly through two pathways (Figure 3c). One pathway was Mongolia–east of the Inner Mongolia–Bohai Sea–Yellow Sea–East China Sea, and the DL sampling site was right on this pathway as shown in Figure 3c. The other pathway was western XinJiang–Mongolia–Inner Mongolia–Loess Plateau–Bohai Sea–Yellow Sea–East China Sea. Nevertheless, there was no explicit evidence of which pathway influenced more on SH by only using the backward trajectory analysis, which will be further discussed in section 3.2.2. A 4 day forward trajectory was applied to TZ in the Taklimakan Desert. It could be seen clearly that the air masses that started at the height of 2000 m had the capability to reach SH. Anyway, it probably had minor influence on the ground aerosol as it reached Shanghai at a high level of ~3000 m. The other two air masses crossed the center of China and then moved out over Korea and Japan, finally ending at the North Pacific Ocean.

3.2.2. Source Identification by Elemental Tracers

[11] Although the air mass trajectory analysis has shed some light on the source of the dust, it is still not very evident to some extent. Here the elemental tracer analysis is used to further characterize the source of the dust. The elemental ratio of Ca/Al has been proven to be an efficient and feasible way [*Sun et al.*, 2005; *Wang et al.*, 2005a] as different dust regions in China are characterized of different Ca content and Ca/Al ratios in soil/particles [*Zhang et al.*, 1996, 2003]. The Ca/Al ratios of all sites during the dust days in this study with previous literature references are listed in Table 2. The Ca/Al ratio of TZ was 1.56 ± 0.14, the highest among all sites and was the typical sign of the western high-Ca-dust source, which was characterized by high Ca content [*Zhang et al.*, 1996]. The ratio of YL was 1.09 ± 0.13, close to the northwestern high-Ca-dust source [*Zhang et al.*, 1996; *Cao et al.*, 2008]. This corresponded well with the backward trajectory analysis above. The lowest Ca/Al value of 0.52 ± 0.05 was observed in DL and it was very close to that in Hunshandake desert [*Zhang et al.*, 1996], which indicated that the dust aerosol over DL was from the northeastern source. The Ca/Al ratio of SH was 0.67 ± 0.20, which was a little higher than that in DL but much lower than that in TZ. Thereby, the dust storm in SH should be more attributed to the dust from the northeastern

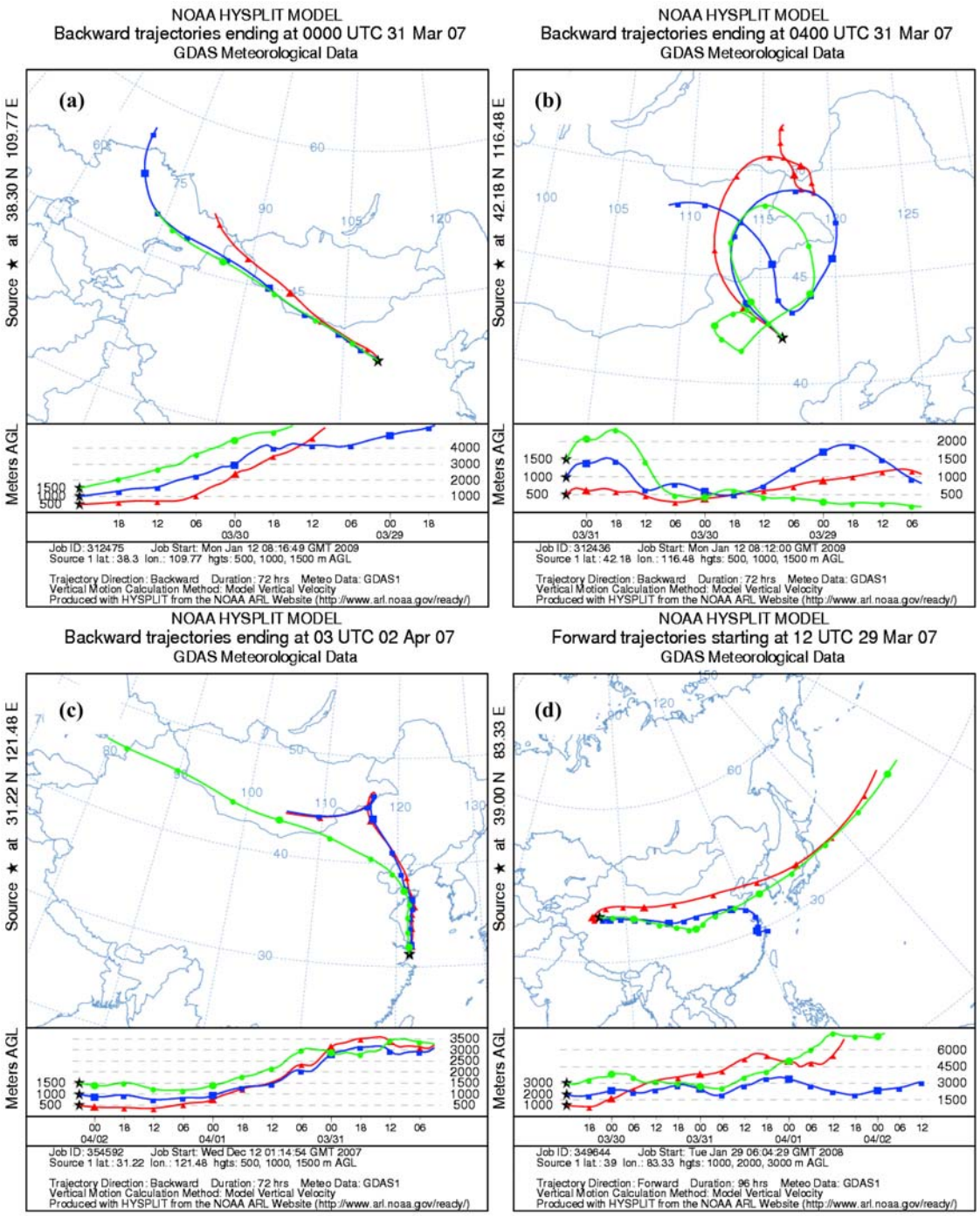

Figure 3. The 3 day backward air trajectories for the dust in (a) YL, (b) DL, and (c) SH and (d) the 4 day forward trajectory in TZ.

source than from the western high-Ca-dust source. In summary, three dust sources were identified: the western high-Ca-dust source and the northwestern high-Ca-dust source with TZ and YL, respectively, as the representative sites. The northeastern low-Ca-dust source was represented by DL. SH could be regarded as the receptor downstream site and mostly from the northeastern low-Ca-dust source in the dust episodes of 2007.

3.3. Chemical Characterization of Dust Aerosol

3.3.1. Elements

[12] Enrichment factor analysis is used here to evaluate the enrichment extent of various elements in aerosol. Usually Al is used as the reference element. The calculation formula is $EF_x = (X/Al)_{aerosol}/(X/Al)_{crust}$, of which X is the element of interest. Species with EFs less than 10 are usually considered to have a major natural crustal source, while

Table 2. Elemental Ratios of Ca/Al at Four Sites During the Dust Storms[a]

Site	Type	Ca/Al	Reference
TZ	TSP	1.56 ± 0.14	This study
YL	TSP	1.09 ± 0.13	This study
DL	TSP	0.52 ± 0.05	This study
SH	TSP	0.67 ± 0.20	This study
Taklimakan Desert			
Western high dust sources	Aerosol	1.99	*Zhang et al.* [1996]
Badain Juran desert			
Northern west high dust sources	Aerosol	1.20	*Zhang et al.* [1996]
Hunshandake sand land		0.52	*Zhang et al.* [1996]
Tongliao, Horqin sand land	$PM_{2.5}$	0.76	*Shen et al.* [2007]
Loess Plateau	Aerosol	1.14	*Zhang et al.* [2003]
	TSP	1.22	*Cao et al.* [2008]
Gobi Soil	<100 mm	1.17	*Ta et al.* [2003]
Yulin, China	$PM_{2.5}$	1.00	*Arimoto et al.* [2004]

[a]The ratios of Ca/Al at other places from literature are listed for comparison.

species with higher EFs are probably contaminated by anthropogenic sources. Average EFs of all the measured elements at four sites were calculated and they could be categorized into three groups. The first group, which included Al, Ca, Co, Cu, Fe, Mg, Mn, Na, Ni, P, Sr, Ti, and V with EFs less than 10, represented the mineral source from crust. The second group consisted of Pb, Zn, and Cd with EFs larger than 10 and less than 100, indicating that these elements were moderately enriched and they could be from both crustal and pollution sources. The last group with As and S had EFs larger than 100, indicating these two elements were highly enriched and mostly from pollution sources. The EFs of most elements followed the order of SH > YL ≈ DL > TZ, indicating the aerosol of TZ was least polluted among four sites. Pb and Zn were found with low EFs less than 10 in TZ, while these two elements were definitely the highly polluted elements at the other three sites, where the EFs of Pb and Zn were tenfold to hundredfold higher than that of TZ. Both Pb and Zn showed good correlations with Al in both ND and DS in TZ (correlation coefficient R = 0.90 for Pb and R = 0.87 for Zn during the whole sampling period), indicating that these two "pollution" elements could be partially from the crustal source. The average mass ratios of Pb in TSP in ND and DS samples collected from TZ were 5.27×10^{-5} and 2.48×10^{-5}, respectively, about 3.8 and 1.8 times of its crustal ratio (1.40×10^{-5}), while the ratios of Zn in ND and DS were 2.24×10^{-4} and 1.03×10^{-4}, respectively, about 3.2 and 2.5 times of its crustal ratio (7.00×10^{-5}). At other sites, the ratios were usually tens or hundreds of times higher. This further indicated that in the source region of the Taklimakan Desert, the "pollution" element had a significant mineral source. To evaluate the contribution of the noncrustal source to the element, the mass concentration of the noncrustal part is calculated by using the formula: $X_{noncrustal} = X_{total} - Al_{aerosol} \times (X/Al)_{crust}$, where X is the element of interest and $(X/Al)_{crust}$ is the ratio of element X to Al in crust. The concentrations of Pb and Zn from noncrustal sources in ND and DS are shown in Figure 4. Noncrustal Zn did not vary greatly between ND and DS in TZ, YL and DL, suggesting a relatively similar background crustal source of Zn. While in SH, the average concentration of noncrustal Zn in DS reached 1.7 $\mu g/m^3$, about 1.5 times that of ND. The increased Zn was probably entrained by the dust during its long-range transport. In the case of Pb, the noncrustal Pb had an obvious increase during DS compared to ND at all sites. The difference between Zn and Pb indicated that nearby the dust sources Zn could have the similar crustal background source, while Pb could be mostly derived from medium- or long-range transport as leaded gasoline has been used widely in the early periods of automobile industries in China and the deposition of the aerosol Pb could have been a regional problem.

[13] Aerosol in TZ was least polluted as discussed above. However, it was found that the element As was moderately enriched with EFs of 51 and 35 in ND and DS, respectively. This probably indicated that even in the source region of the dust, the mixed aerosol; that is, the mixing of minerals with pollutants had already existed. The enrichment of As probably derived from coal burning as coal and natural gases are widely used in Xinjiang Autonomous Municipality. The pollution contamination in the source region of dust had also been found previously in northwestern China [*Arimoto et al.*, 2004; *Xu et al.*, 2004] and in the eastern Mediterranean dust region [*Erel et al.*, 2006].

[14] The ratios of concentrations and EFs of all elements in DS versus ND are shown in Figure 5. The concentrations of Al, Ca, Fe, Mg, Co, Mn, Na, P, Sr, Ti, and V increased 8~30 times during the dust days compared to the nondust days and those of As, Cd, Cu, Pb, Zn and S were also elevated 1~8 times. The results indicated that the dust storm not only brought abundant minerals but also pollutants. The highest increase was observed in SH and this implied that the dust storm had the greatest impact on the downstream regions, which were even far away from the dust source. Part of the pollutants brought by the dust could also be from the medium-range or regional transport from Beijing and Shandong Province (northern China) based on the backward trajectories. The ratios of EFs of DS versus those of ND for those pollution elements were all below 1.00, indicating the dilution of the anthropogenic pollutants by the dust during the dust storm days.

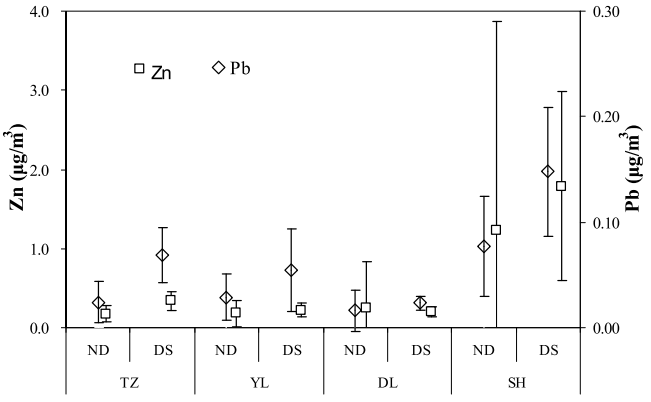

Figure 4. The concentrations of noncrustal Pb and Zn in nondust (ND) and dust storm (DS) periods at four sites; error bar represents 1 standard deviation.

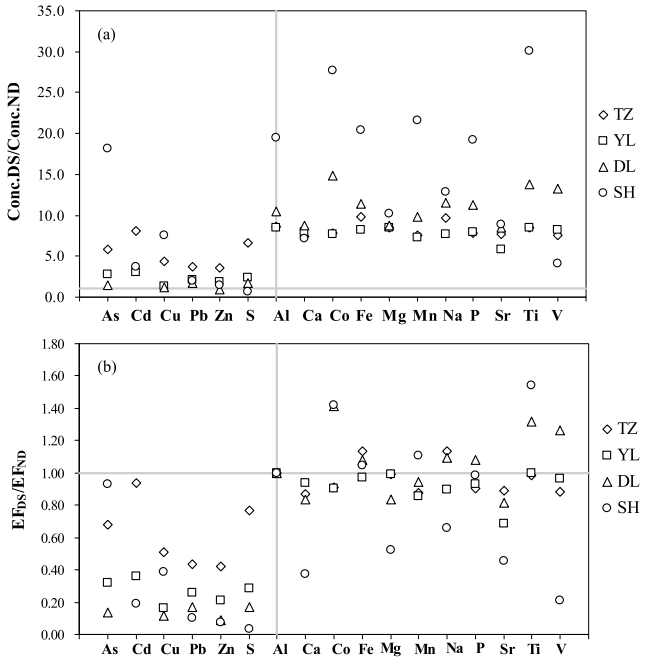

Figure 5. (a) The ratios of the concentrations in DS to those in ND ($Conc._{DS}/Conc._{ND}$). (b) The ratios of EFs of all the elements in DS to those in ND (EF_{DS}/EF_{ND}).

3.3.2. Soluble Ions

[15] The ratios of the concentrations of the major soluble ions in DS to those in ND ($Conc._{DS}/Conc._{ND}$) are shown in Figure 6. Na^+, K^+, Mg^{2+}, and Ca^{2+}, i.e., the mineral ions, all unexceptionally increased during DS (Figure 6a). The ratios of TSP were higher than those of $PM_{2.5}$ at the dust source regions, i.e., TZ, YL and DL. While at the coastal site of SH, the ratio of $PM_{2.5}$ was much greater than that of TSP. This could suggest that the dust impact more on those coarse particles in dust source regions, while the dust would impact more on the fine particle in the downstream regions due to the dry deposition of coarse particles. The mass percentages of Na^+, K^+, Mg^{2+}, and Ca^{2+} in TSP in DS were similar to those in ND at TZ. While at the other sites, the mass percentages of these soluble ions in aerosol were 2~5 times lower in DS compared to those in ND. Given that TZ is in the middle of the Taklimakan Desert and there are no significant anthropogenic sources in the surrounding areas, the similar composition of aerosol between DS and ND are expected. While at other sites, more insoluble components would be entrained by the dust, which decreased the mass percentage of those mineral ions, i.e., Na^+, K^+, Mg^{2+}, and Ca^{2+}.

[16] The ions, which normally were included in the category of pollution ions and from so-called "secondary aerosol," showed different behaviors among SO_4^{2-}, NO_3^- and NH_4^+ (Figure 6b). It must be noted that the concentrations of SO_4^{2-}, like the mineral ions, increased during the dust storm at all sites. At the sampling site of the Taklimakan Desert (TZ), the average concentrations of SO_4^{2-} in $PM_{2.5}$ and TSP during DS were 36.0 and 109.3 $\mu g/m^3$, while they were 8.3 and 15.0 $\mu g/m^3$ during ND, respectively. It must be noted that although SO_4^{2-} in $PM_{2.5}$ and TSP during DS was about 4.3 and 7.3 times of that during ND, the contribution of SO_4^{2-} to the total mass of $PM_{2.5}$ and TSP varied just a little with the average mass percentage of 3.97% and 2.81% in $PM_{2.5}$ and TSP during ND, and 3.53% and 2.53% in $PM_{2.5}$ and TSP during DS, respectively. The total S content in the surface soil collected from many places in the Taklimakan Desert was much higher than its average world crustal abundance. For instance, the S content in the surface soil collected from TZ was 0.125%, about 4 times of the average crustal abundance of 0.035% [*Nishikawa et al.*, 1991], while the Al content in the surface soil collected from TZ was 4.52%, much lower than that of the average crustal abundance of 8.13%. If using the ratio of S/Al in the surface soil of TZ as reference, the enrichment factor of S in $PM_{2.5}$ and TSP during DS was 7.6 and 7.0, while it was 9.0 and 8.6, respectively, during ND. It should be emphasized that the ratios of water soluble sulfur content in sulfate to the total sulfur; that is, S in SO_4^{2-} to the total sulfur (SO_4^{2-}/S) in $PM_{2.5}$ and TSP was 0.88 and 0.91, respectively, clearly suggesting that sulfur in $PM_{2.5}$ and TSP was mostly (88–91%) in the form of sulfate. It was also worthy to note that SO_4^{2-} correlated very well with Na^+, Cl^-, and Ca^{2+} ($R > 0.97$), indicating that they likely have the common source. All of these features suggested that the sulfate in the dust aerosol over TZ, the center of Taklimakan desert, was mostly from the "crustal" source, i.e., from the emitted primary dust aerosol, instead of the secondary aerosol formed from the chemical reactions of

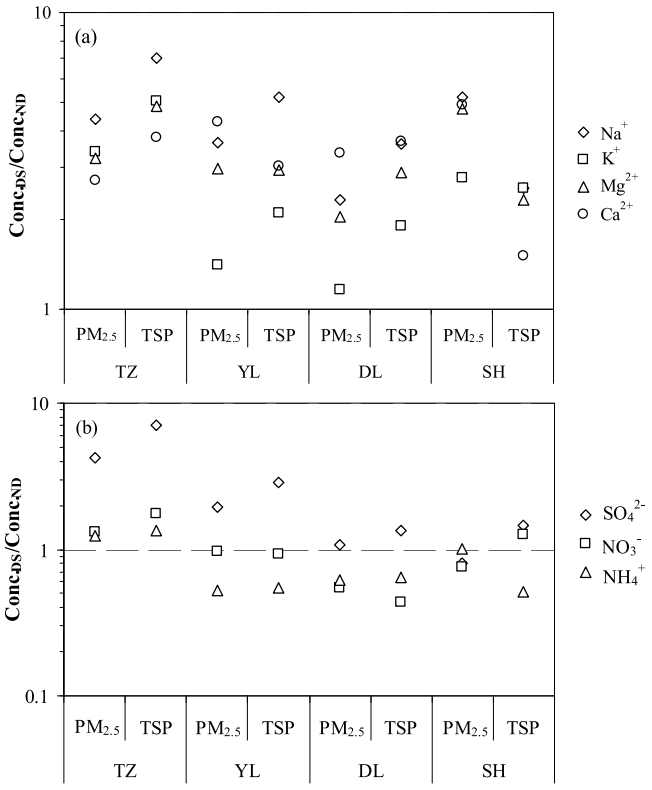

Figure 6. The ratios of the concentrations of major soluble ions in DS to those in ND in TSP (a) Na^+, K^+, Mg^{2+}, and Ca^{2+} and (b) SO_4^{2-}, NO_3^-, and NH_4^+.

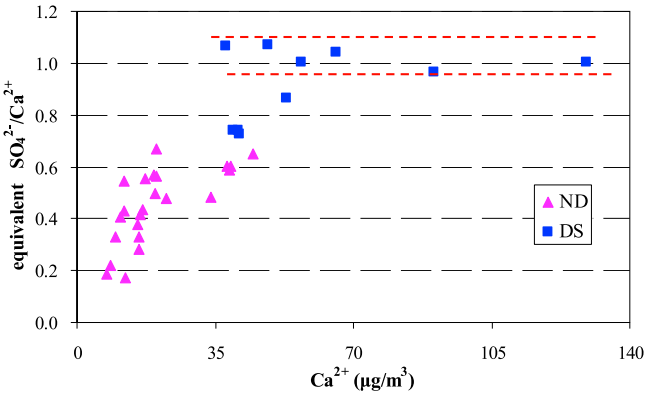

Figure 7. The equivalent ratios of SO_4^{2-}/Ca^{2+} versus the concentrations of Ca^{2+} at TZ.

the anthropogenic SO_2. As the Taklimakan Desert was speculated to be ocean 5–7 millions years ago [*Sun and Liu*, 2006], the dried sea salts from the paleo-ocean should be the major source of the aerosol of TZ. That's the reason why the sulfate aerosol of the Taklimakan Desert was at such a high concentration level and the mass percentage of sulfate in aerosol varied little between ND and DS.

[17] At the other three sites, i.e., YL, DL, and SH, the concentrations of sulfate increased 1.5~3 times, but its mass percentages decreased 2~7 times during the dust days. Compared to the characteristics of sulfate in TZ mentioned above, the sulfate in the dust particles collected from these three sites probably resulted from the sorption of gaseous SO_2, and the consequent transformation to sulfate aerosol on the surface of dust and could be also due to the mixing of sulfate aerosol with the dust on the pathway of the dust transport [*Arimoto et al.*, 2004]. Figure 6b shows that the increasing ratio of sulfate was higher in TSP than that in $PM_{2.5}$, which meant that the formation of sulfate was more favored in the coarse particles than in the fine particles during dust storm. This maybe indicated that SO_4^{2-} tended to exist in the coarse particle in the form of $CaSO_4$ during dust storm days, while it tended to exist in the fine particles in the form of $(NH_4)_2SO_4$ during nondust days (see discussion in section 3.4). Unlike sulfate, the concentrations of NO_3^- and NH_4^+ remained constant or even decreased in DS compared to ND. The similar phenomenon was also found during the dust storm in Beijing in 2001and 2002 [*Yuan et al.*, 2008]. This implied that the heterogeneous formation of nitrate and ammonium on dust was negligible and these two secondary ions mainly derived from the local sources.

3.4. Mixing Mechanisms

[18] The different origins of dusts, air mass pathways, and mixing mechanisms during the transport are vital factors affecting the concentrations and chemical/optical properties of the aerosol [*Arimoto et al.*, 2006]. The transported dust with the mixing process on the pathway would be sure to change the composition of the aerosols in dust storms [*Zhao et al.*, 2007a], and the transport variability has become a more important factor than the source variability [*Tegen and Miller*, 1998]. Soluble ions took a significant role in the mixing between mineral aerosol and pollution aerosol and this effect was found to be a ubiquitous phenomenon during the dust seasons [*Wang et al.*, 2005a].

[19] In TZ, SO_4^{2-} had a strong relation with Al in TSP during both ND and DS (R = 0.94). This indicated sulfate had a significant primary source, i.e., the paleo-ocean dried sea salts in the Taklimakan Desert as mentioned above. The possible existence forms of sulfate could be $CaSO_4$, Na_2SO_4, K_2SO_4, and $MgSO_4$. Although good correlations were found between SO_4^{2-} and all the major cations, of which only the equivalent ratio of Ca^{2+}/SO_4^{2-} was close to unity, indicating that the major part of SO_4^{2-} maybe existed in the form of $CaSO_4$. Figure 7 plots the equivalent ratios of SO_4^{2-}/Ca^{2+} against the concentrations of Ca^{2+}. When the concentrations of Ca^{2+} reached a certain value (>50 $\mu g/m^3$), the equivalent ratios of SO_4^{2-}/Ca^{2+} approached 1.00. This suggested that in the high dust, which was distinguished by the high Ca^{2+} concentrations, the dissolved part of the dust almost contained the equal moles of SO_4^{2-} and Ca^{2+}. The main form of SO_4^{2-} and Ca^{2+} in the dissolved part of the dust storm of TZ seemed to be gypsum/anhydrite ($CaSO_4$). While in the low dust, the equivalent ratio of SO_4^{2-}/Ca^{2+} was less than 1.00, which meant that sulfate couldn't account for the total Ca^{2+}. Apart from the contribution of gypsum to the total Ca^{2+}, the remaining water soluble Ca^{2+} probably existed in the form of calcium carbonate ($CaCO_3$). The SO_4^{2-}/Ca^{2+} ratios increased with the increase of the Ca^{2+} concentrations, which meant the higher dust brought more $CaSO_4$ than $CaCO_3$. As for NO_3^-, it was found to be moderately correlated with NH_4^+. The average concentrations of NO_3^- and NH_4^+ in TZ were 2.26 and 0.99 $\mu g/m^3$, respectively, which were at very low concentration levels among four sites. In the desert, there is very little population of humans and animals, and consequently few anthropogenic sources. Very few NO_x emissions and the human/animal excrement may be responsible for such a low level of NO_3^- and NH_4^+ in TZ.

[20] In YL, no correlation was found between SO_4^{2-} and Al in ND and the average mass percentage of SO_4^{2-} in TSP in DS was 1.97%, much higher than that in the surface soil of 0.01%. In this regard, sulfate in YL seemed to be dominated by the anthropogenic source in both ND and DS. From Figure 8a, SO_4^{2-} correlated well with NH_4^+ in ND with the correlation coefficient of 0.74, while there was no such positive correlation in DS. The concentration of SO_4^{2-} increased with the decrease of NH_4^+ as visualized by the dashed line in Figure 8a. As indicated above, NH_4^+ mainly derived from the local sources and the entrained dust contained little ammonium. NH_4^+ would be diluted when the dust invaded, and the dilution of NH_4^+ would be more pronounced as the dust increased which was accompanied with higher concentrations of SO_4^{2-}. The peak value of SO_4^{2-} during the dust storm days reached 47.03 $\mu g/m^3$, which was about 6 times the average concentration in the nondust days. YL is at the edge of the northern part of Shanxi Province, where many large coal mines are located. The extensive coal usage for heating and cooking may be one of the most important sources of local pollutants in Yulin [*Hou et al.*, 2006; *Xu et al.*, 2004]. SO_4^{2-} in the dust particles could result from the sorption of gaseous SO_2 and the reaction with the alkaline components in the dust, such as $CaCO_3$. Therefore the mixing of sulfur from the coal mines with the alkaline dust was a reasonable explanation for why SO_4^{2-} showed such high concentrations during the dust storm

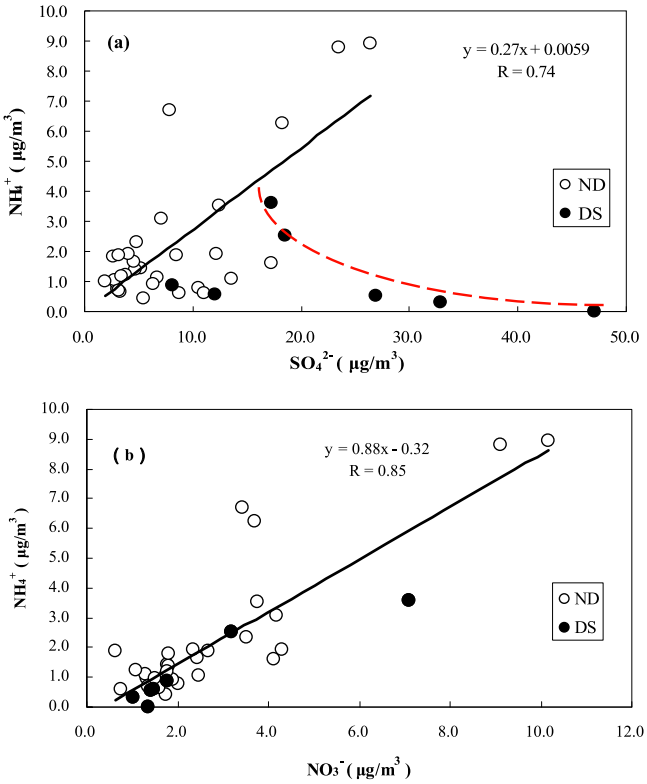

Figure 8. The correlation between (a) SO_4^{2-} and NH_4^+ and (b) NO_3^- and NH_4^+ at YL in ND and DS. Linear fits between two species are plotted, and the dashed line in Figure 8a is for visual reference.

days. In the case of NO_3^-, it correlated with NH_4^+ in both ND and DS (Figure 8b), which showed the different behavior compared to SO_4^{2-}. The reaction rates for nitrate production on dust were strongly dependent on the relative humidity. Generally, dust-laden air is quite dry [*Arimoto*, 2001] and O_3, NO_2, and HNO_3 were found to decrease by up to 20%, 20%, and 95%, respectively, in terms of model study during the ACE-Asia Experiment [*Tang et al.*, 2004]. The low temperature, relative humidity, strong wind and the low-pollution gases did not benefit the photochemical reaction, the NOR (nitrogen oxidation ratio) was low and even less than 1% during the dust storm of Beijing [*Yuan et al.*, 2008]. That could explain why nitrate behaved differently from sulfate during DS. NO_3^- and NH_4^+ were more physically affected by the dust storm, i.e., the dilution effect, rather than the chemical reaction on the dust. Thus good relationship could still be observed between these two species during DS.

[21] In DL, the formation mechanism of sulfate and nitrate was similar as that in YL (not shown Figure 8b). The concentrations of the two pollution ions, SO_4^{2-} and NO_3^-, were the lowest among the four sites. Additionally, the average concentration of SO_4^{2-} in DS was only slightly higher than that in ND, probably indicating the heterogeneous reaction there was not prominent. As DL is close to one of the major sources of Asian dust in the eastern Mongolia Gobi, and no obvious anthropogenic sources are on the transport pathway of the dust, there were few chances for the mixing of dust with pollutants prior to the sampling at this site, so the mixing extent was not obvious.

[22] The most severe pollution was found in SH. In the nondust days, the average concentrations and mass percentages of SO_4^{2-} and NO_3^- in aerosol were the highest among the four sites. The sum of SO_4^{2-} and NO_3^- accounted for an average of 35% and 21% of the total mass of $PM_{2.5}$ and TSP, respectively. Coal burning and vehicle emission were two main anthropogenic sources in Shanghai [*Wang et al.*, 2006a]. To explore their formation mechanisms, we analyzed the relationship between SO_4^{2-} and NO_3^- and $NH_4^+$and Ca^{2+}. Surprisingly, no significant correlations were found in any of the mutual two species, which maybe indicated that neither NH_4^+ nor Ca^{2+} could dominate the neutralization process of the two acids. Alternatively, the sum of the equivalent concentrations of NH_4^+ and Ca^{2+} versus those of SO_4^{2-} and NO_3^- was plotted (Figure 9) and good relation was observed in ND with the correlation coefficient of 0.78. The average equivalent ratio of $[NH_4^+ + Ca^{2+}]/[SO_4^{2-} + NO_3^-]$ in ND was 1.09, very close to unity, indicating that the alkaline components could just fully neutralize the acids. While in DS, the average ratio decreased to 0.82, probably suggesting that although the dust brought abundant alkaline components, the acidity in SH aerosol still could not be completely neutralized. It was found that the average concentration of NO_3^- increased from 9.67 $\mu g/m^3$ in ND to 12.31 $\mu g/m^3$ in DS. In addition, the average concentration of MSA (methylsulfonic acid) in DS increased several times compared to that in ND. As MSA was an indicator of the marine source, this implied that the dust plumes probably took the passage on the sea before arriving at Shanghai, which could also be supported by the back trajectory analysis (Figure 3c). Previous studies have found that on the west coast of Japan during an Asian dust storm event, 79% of total particle population was found to be modified by sea salt through the individual particle analysis [*Ma et al.*, 2005] and the interaction of dust with sea salt was likely an important process in size and composition changes of dust aerosols during their long-range transport [*Zhang and Iwasaka*, 2004]. This could explain why an evident increase of nitrate was only found in SH during the dust days (Figure 6b), and we attributed this to

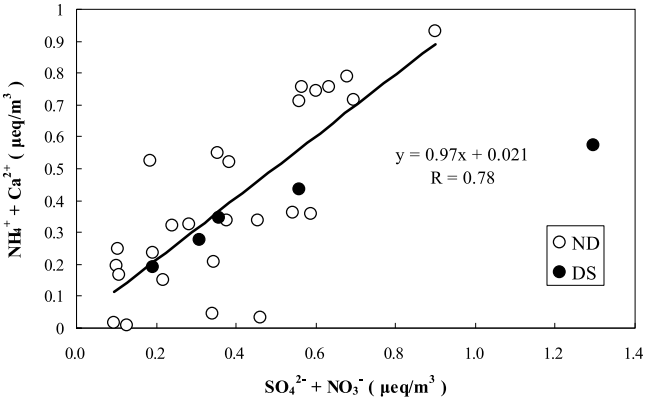

Figure 9. The correlation between the equivalent concentrations of $[SO_4^{2-} + NO_3^-]$ and $[NH_4^+ + Ca^{2+}]$ in SH in ND and DS. Linear fit is plotted for ND.

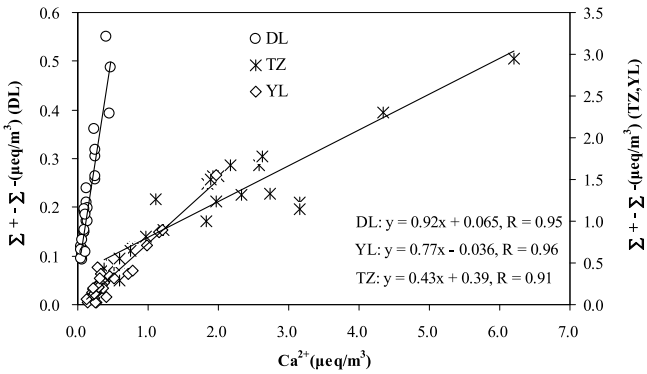

Figure 10. The relationship between the deficiency of anions ($\sum+ - \sum-$) and the equivalent concentrations of Ca^{2+} in TZ, YL, and DL.

the heterogeneous reaction between sea salt and the precursors of nitrate. Thus, the mixing mechanism in SH probably involved the interaction of dust, sea salt, and local pollutants. The lowest pH value of the dust sample filtrate reached as low as 2.81, about 2 pH units lower compared to the nondust samples, which was the strong evidence that the long-range transport of the dust brought much more acidic ions, such as SO_4^{2-} and NO_3^-, to Shanghai. While at the other sites, the pH values of the dust samples were usually higher than those of the nondust samples due to the high alkalinity of the dust. During the 2001 TRACE-P flight observations, the pH of the dust that transported over Shanghai also reached a low value of approximate 1.00 calculated from the concentrations of the trace gases, including HNO_3(g), in the air and the components in the dust aerosol [*Meskhidze et al.*, 2003]. The high acidity of the dust aerosol could be explained by the severe local pollution in Shanghai plus those acidic ions brought by the invaded dust aerosol, which mixed and interacted with those pollution precursors on the transport pathway before arriving at Shanghai, although the dust could neutralize part of those acidic components. From Figure 6a, it could be seen that the increasing amount of Ca^{2+} in TSP in SH was the lowest among all sites. During the long-range transport, large particles were usually subject to the dry deposition, which would greatly reduce the neutralization extent of the pollution acidic components in the aerosol. Additionally, the production of sulfate and nitrate was enhanced by the heterogeneous reactions on the mineral dusts and sea salts. Thereby, high acidity in dust aerosols was observed in Shanghai.

3.5. Speciation of the Soluble Ions

[23] A major objective of this study is to characterize and compare the species of the Asian dust from different sources and to see the variability of the species during the long-range transport. The ratios of the total equivalent cations ($\sum+$) to the total equivalent anions ($\sum-$) of TZ, YL and DL were all higher than unity in both ND and DS. As ion chromatography is unable to measure CO_3^{2-}, the unbalanced anion was assumed to be CO_3^{2-} as carbonate was a primary contributor to the surface soil and aerosol in the northern and western China [*Wang et al.*, 2008; *Cao et al.*, 2008]. While in SH, the $\sum+/\sum-$ ratio was less than unity in both ND and DS, indicating aerosols in SH were more acidic than those at the other sites. In order to explore the existing form of the unbalanced ions, the deficiency of anions calculated by ($\sum+ - \sum-$) is plotted against the equivalent concentrations of Ca^{2+} in TZ, YL and DL (Figure 10; SH is not shown in Figure 10 as almost no anion deficiency was observed there). The strong correlations between the two variables indicated that CO_3^{2-} probably existed in the form of calcium carbonate as $CaCO_3$, which was a ubiquitous component in soils from various arid and semiarid areas in northern and western China. Thus, we estimated the mass concentration of $CaCO_3$ by using the formula of $[CaCO_3] = (\sum+ - \sum-) \times 100$, where 100 is the molecular weight of $CaCO_3$. With all the major soluble ions clarified, we could roughly estimate the concentrations of species [*Wang et al.*, 2005b, 2006b] with the correlation analysis. The major species in both ND and DS at all sites and the mass percentages of the major species in total soluble ions are shown in Figure 11. Ca^{2+} was mainly in the form of calcium carbonate (calcite) and calcium sulfate (gypsum and anhydrite) [*Mikami et al.*,

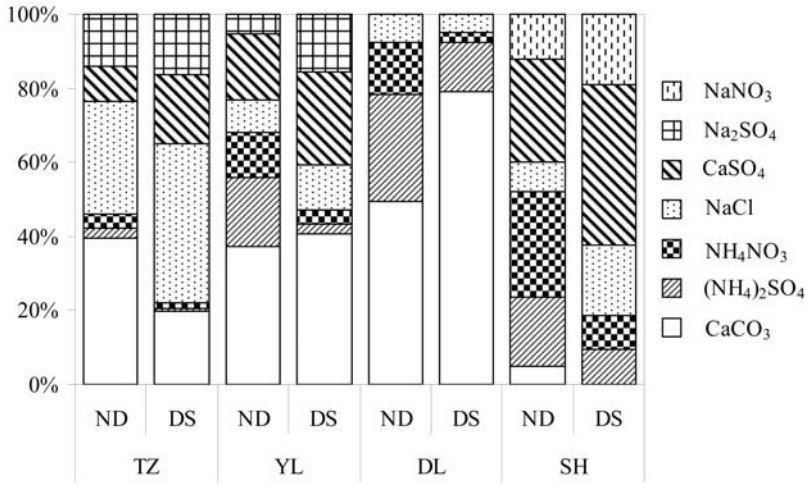

Figure 11. The mass percentages of the major species in the total soluble ions in ND and DS at four sites.

Table 3. Ratios of S in SO_4^{2-} to Total S, Ca^{2+} to Ca, and Na^+ to Na in ND and DS at Four Sites

	ND or DS	TZ	YL	DL	SH
SO_4^{2-}/S	ND	0.89 ± 0.16	1.00 ± 0.18	0.73 ± 0.10	1.00 ± 0.17
	DS	0.97 ± 0.12	1.00 ± 0.10	0.54 ± 0.09	1.00 ± 0.17
Ca^{2+}/Ca	ND	0.37 ± 0.09	0.77 ± 0.13	1.00 ± 0.18	1.00 ± 0.29
	DS	0.19 ± 0.05	0.33 ± 0.09	0.41 ± 0.10	0.49 ± 0.03
Na^+/Na	ND	1.00 ± 0.30	0.88 ± 0.19	1.00 ± 0.20	1.00 ± 0.34
	DS	0.79 ± 0.11	0.61 ± 0.16	0.27 ± 0.03	0.25 ± 0.06

2006]. Clearly, calcite was one of the main contributors to the total ions in both ND and DS in the three dust source regions, i.e., TZ, YL and DL, while it contributed less than 10% of the total soluble ions in SH. Carbonate could greatly affect atmospheric chemical processes and the characteristics of aerosols because it serves as a substrate for adsorbing SO_2 or sulfuric acid and facilitating the heterogeneous conversion of sulfur dioxide to be sulfate [*Dentener et al.*, 1996; *Yuan et al.*, 2006]. Obvious increased mass fraction of $CaSO_4$ was observed in TZ, YL, and SH during the dust storm days, and the formation mechanism of sulfate has been elaborated in the discussion above.

[24] SH was directly influenced by the dust plumes from DL, as indicated from the back trajectory analysis (Figure 3c), the long-range transport of the dust aerosol from DL would induce the evolution of the aerosol composition on the pathway. The composition of aerosols in DL and SH was observed to be completely different. The main species in the aerosol over DL were calcite, secondary species (mainly ammonium sulfate) and halite (sodium chloride). The presence of $(NH_4)_2SO_4$ and the absence of $CaSO_4$ in DL suggested that the heterogeneous reactions could be almost neglected there. Compared to the high content of $CaCO_3$ (~80% in dust storm days) in the total soluble part of DL aerosol, we found high content of $CaSO_4$ in the total soluble part in SH aerosol (43% in the dust storm days) and the absence of $CaCO_3$. During the long-range transport, the high carbonate in the dust from DL to SH had been fully neutralized by the high concentration of acidic species, such as SO_2 or its oxidation products (SO_3 and H_2SO_4(g)), as almost all $CaCO_3$ in the total soluble part of dust from DL was transformed to $CaSO_4$ and almost no $CaCO_3$ was found in the aerosol in SH during the dust storm days. The mass percentage of $CaSO_4$ in the total soluble ions in SH increased from 27% in ND to 43% in DS and the average SO_4^{2-}/Ca^{2+} ratio increased ~6 times in SH compared to that in DL, which implied the strong mixing and transformation process from $CaCO_3$ to $CaSO_4$ during the long-range transport from DL to SH. The existence of $NaNO_3$ and its prominent increase during the dust storm days also supported the mixing and transformation process of dust with sea salts and pollutants in SH. It was sure that the long-range transport of dust aerosol would change the particle number, size distribution and chemical composition of the dust and furthermore its optical properties.

[25] $(NH_4)_2SO_4$ and NH_4NO_3 were among the major secondary species during the nondust days in YL and SH. Coal usage, power plants and vehicle emissions were responsible for the precursors of SO_4^{2-} and NO_3^-. The abundances of $(NH_4)_2SO_4$ and NH_4NO_3 were controlled by the amount of NH_4^+. During the dust storm days, the contributions of these two species were suppressed to a low fraction due to the dilution of NH_4^+ by the invaded dust. Sodium chloride existed at all sites. Na^+ and Cl^- correlated very well with the correlation coefficient of 0.99 in TZ because the dust over the Taklimakan Desert had its paleomarine source. NaCl in YL and DL probably derived from the saline minerals as there were dried salt lakes or saline soils in northern China and southern Mongolia [*Yuan et al.*, 2006]. The sodium and chloride in SH was obviously from the marine source, and the increased contribution of NaCl to the total ions in DS further implied the mixing of the dust with sea salts during the long-range transport of the dust aerosol.

3.6. Tracers for Distinguishing Different Dust Sources

[26] There have been various tracers used to address the provenance of the dust particles, such as isotopic methods [*Arimoto*, 2001], iron oxide [*Shen et al.*, 2006] and clay ratios [*Caquineau et al.*, 1998]. New tracers were explored for distinguishing the different dust sources in this study. The ratio of Ca/Al is a good tracer in distinguishing the different dust sources over China, which was discussed in section 3.2.2. In addition to the Ca/Al tracer, the ratios of SO_4^{2-}/S, Ca^{2+}/Ca and Na^+/Na in DS and ND, which are listed in Table 3, could also be used to identify the sources of dust aerosols.

[27] In YL, sulfur almost existed in the soluble form, i.e., sulfate, in both ND and DS. As mentioned above, the major source of sulfur in YL was from the coal mines and the products of sulfur dioxide through homogeneous or heterogeneous reactions were mainly $(NH_4)_2SO_4$ and $CaSO_4$, which were highly water soluble salts. Most of the sulfur in TZ also existed in the soluble state, mainly in $CaSO_4$ and Na_2SO_4. The dust from northeastern China (DL to be the representative) seemed to have the lowest fraction of soluble sulfur (0.54) in the aerosol compared to the other two dust sources, western and northwestern China (TZ (0.97) and YL (1.00) to be the representatives of these two sources). The insoluble sulfur perhaps derived from the iron pyrites (FeS_2) or copper pyrites ($CuFeS_2$) as these mines were located in many places in Inner Mongolia. The soluble fraction of sulfur in DL decreased from 73% in ND to 54% in DS, indicating the dust could transport more insoluble materials. In SH, all sulfur was in the soluble part in ND, which was mainly due to that it was almost all formed from secondary aerosol. Although influenced by the dust plume from the northeast, the fraction of sulfur in the soluble part in DS still approached 100%. This indicated that there was chemical reaction that transformed insoluble sulfur to soluble sulfur during long-range transport.

[28] Ca^{2+}/Ca ratios (Table 3) in ND were higher than those in DS at all sites, indicating that the dust could bring more insoluble Ca. The insoluble Ca mainly existed as mica/Ca silicates bound in mineral structures [*DeBell et al.*, 2004]. The Ca^{2+}/Ca ratios followed such sequence as TZ < YL < DL < SH, indicating the increase of the water soluble Ca from the west to the east. The dust from TZ derived from the very inner part of the Taklimakan Desert, where the sand particles contained more insoluble components. While the dust traveled in YL, DL and SH, it was more or less impacted by the local mineral source, which contained higher fractions

of soluble Ca, thus, the ratio of Ca^{2+}/Ca in dust storm days increased from 0.19 in TZ to 0.33 in YL, 0.41 in DL, and 0.49 in SH. The Ca^{2+}/Ca ratio in SH was close to that in DL during the dust days, which further confirms that the dust in SH was mostly influenced by the northeastern dust source (DL as the representative). It can be seen from the ratios of Na^+/Na that sodium existed almost 100% in the form of water soluble part in ND at all sites, for the sodium in each site mainly derived from the local soils or marine source during nondust days. In the dust storm days, the ratio of Na^+/Na at each site followed the order of TZ > YL > DL ≈ SH, which was the opposite compared to ratio of Ca^{2+}/Ca. The insoluble Na perhaps existed in its crystalline form and the dust from the northeastern source (DL) could bring more insoluble Na than the other two dust sources (TZ and YL). The Na^+/Na ratios in DL (0.27) and SH (0.25) were very similar in DS, again demonstrating that the dust in SH was mostly from the northeastern dust source.

[29] In summary, the western high-Ca dust (the Taklimakan Desert, TZ as the representative) is characterized with high ratio of Ca/Al plus higher Na^+/Na and lower Ca^+/Ca, while the northeastern low-Ca dust (Eastern Mongolia Gobi, DL as the representative) is characterized with low ratio of Ca/Al plus lower Na^+/Na and higher Ca^+/Ca. The characteristics of northwestern high-Ca dust (Western Mongolia Gobi, YL as the representative) are intermediate between the two dust sources mentioned above. These characteristics provide another very useful tools for tracing the origins of Asian eolian dusts.

4. Conclusions

[30] 1. Three Asian dust sources, i.e., the western high-Ca dust in the Taklimakan Desert, the northwestern high-Ca dust and the northeastern low-Ca dust in Mongolia Gobi, were identified based on the air mass trajectories plus the elemental tracer analysis (e.g., Ca/Al, SO_4^{2-}/S, Ca^{2+}/Ca and Na^+/Na). The western dust source was least polluted in comparison to the other two dust sources. The results evidently indicated that the dust could have already mixed with pollution aerosol even near dust source regions.

[31] 2. Asian dust not only brought high concentration of minerals to the downstream areas, but also much pollution. The concentrations of As, Cd, Cu, Pb, Zn, and S were elevated several times at all sites during dust days, showing the entrainment of pollution elements by dust. The secondary SO_4^{2-} was observed to show much higher concentration due to the heterogeneous reaction on the alkaline dust during dust storms, while the concentrations of NO_3^- and NH_4^+ decreased due to the dilution of the local pollution by the invaded dust.

[32] 3. The western dust involved less anthropogenic aerosol, and it mainly derived from the Taklimakan Desert, a paleomarine source. The northwestern dust had a considerable mixing and chemical reaction with sulfur precursors from the coal mines on the pathway of the long-range transport. The northeastern dust reached Shanghai with high acidity, and it became the mixed aerosol with the interaction among dust, local pollutants, and sea salts.

[33] 4. Comparison of the speciation of the water soluble ions in both nondust and dust days at all sites illustrated the ion species from different dust sources and their evolution during the long-range transport. The mixing mechanisms of the dust with the pollution aerosol on the local, medium-range, and long-range scale revealed from this study would improve the understanding of the impacts of Asian dust on regional/global climate change.

[34] **Acknowledgments.** This work was supported by the National Key Project of Basic Research of China (grant 2006CB403704), National Natural Science Foundation of China (grants 20877020, 40575062, and 40599420), and Chinese Desert and Meteorology Study Foundation (grant SQG2005007).

References

Arimoto, R. (2001), Eolian dust and climate: Relationships to sources, tropospheric chemistry, transport and deposition, *Earth Sci. Rev.*, *54*, 29–42, doi:10.1016/S0012-8252(01)00040-X.

Arimoto, R., X. Y. Zhang, B. J. Huebert, C. H. Kang, D. L. Savoie, J. M. Prospero, S. K. Sage, C. A. Schloesslin, H. M. Khaing, and S. N. Oh (2004), Chemical composition of atmospheric aerosols from Zhenbeitai, China, and Gosan, South Korea, during ACE-Asia, *J. Geophys. Res.*, *109*, D19S04, doi:10.1029/2003JD004323.

Arimoto, R., et al. (2006), Characterization of Asian dust during ACE-Asia, *Global Planet. Change*, *52*, 23–56, doi:10.1016/j.gloplacha.2006.02.013.

Bauer, S. E., M. I. Mishchenko, A. A. Lacis, S. Zhang, J. Perlwitz, and S. M. Metzger (2007), Do sulfate and nitrate coatings on mineral dust have important effects on radiative properties and climate modeling?, *J. Geophys. Res.*, *112*, D06307, doi:10.1029/2005JD006977.

Cao, J. J., S. C. Lee, X. Y. Zhang, J. C. Chow, Z. S. An, K. F. Ho, J. G. Watson, K. Fung, Y. Q. Wang, and Z. X. Shen (2005), Characterization of airborne carbonate over a site near Asian dust source regions during spring 2002 and its climatic and environmental significance, *J. Geophys. Res.*, *110*, D03203, doi:10.1029/2004JD005244.

Cao, J. J., J. Chow, J. Watson, F. Wu, Y. Han, Z. Jin, Z. Shen, and Z. An (2008), Size-differentiated source profiles for fugitive dust in the Chinese Loess Plateau, *Atmos. Environ.*, *42*, 2261–2275, doi:10.1016/j.atmosenv.2007.12.041.

Caquineau, S., A. Gaudichet, L. Gomes, M.-C. Magonthier, and B. Chatenet (1998), Saharan dust: Clay ratio as a relevant tracer to assess the origin of soil-derived aerosols, *Geophys. Res. Lett.*, *25*(7), 983–986, doi:10.1029/98GL00569.

Cheng, T., D. Lu, H. Chen, and Y. Xu (2005), Physical characteristics of dust aerosol over Hunshan Dake sandland in Northern China, *Atmos. Environ.*, *39*, 1237–1243, doi:10.1016/j.atmosenv.2004.10.034.

Cheng, Y. F., et al. (2006), Mixing state of elemental carbon and non-light-absorbing aerosol components derived from in situ particle optical properties at Xinken in Pearl River Delta of China, *J. Geophys. Res.*, *111*, D20204, doi:10.1029/2005JD006929.

DeBell, L. J., M. Vozzella, R. W. Talbot, and J. E. Dibb (2004), Asian dust storm events of spring 2001 and associated pollutants observed in New England by the Atmospheric Investigation, Regional Modeling, Analysis and Prediction (AIRMAP) monitoring network, *J. Geophys. Res.*, *109*, D01304, doi:10.1029/2003JD003733.

Dentener, F. J., G. R. Carmichael, Y. Zhang, J. Lelieveld, and P. J. Crutzen (1996), Role of mineral aerosol as a reactive surface in the global troposphere, *J. Geophys. Res.*, *101*, 22,869–22,889, doi:10.1029/96JD01818.

Erel, Y., U. Dayan, R. Rabi, Y. Rudich, and M. Stein (2006), Trans boundary transport of pollutants by atmospheric mineral dust, *Environ. Sci. Technol.*, *40*, 2996–3005, doi:10.1021/es0515021.

Fan, X., K. Okada, N. Nimura, K. Kai, K. Arao, G. Shi, Y. Qin, and Y. Mitsuta (1996), Mineral particles collected in China and Japan during the same Asian dust-storm event, *Atmos. Environ.*, *30*, 347–351, doi:10.1016/1352-2310(95)00271-Y.

Guo, J., A. Kenneth, and G. Zhuang (2004), A mechanism for the increase of pollution elements in dust storms in Beijing, *Atmos. Environ.*, *38*, 855–862, doi:10.1016/j.atmosenv.2003.10.037.

Hou, X., G. Zhuang, Y. Sun, and Z. An (2006), Characteristics and sources of polycyclic aromatic hydrocarbons and fatty acids in PM2.5 aerosols in dust season in China, *Atmos. Environ.*, *40*, 3251–3262, doi:10.1016/j.atmosenv.2006.02.003.

Kim, K. W., Z. He, and Y. J. Kim (2004), Physicochemical characteristics and radiative properties of Asian dust particles observed at Kwangju, Korea, during the 2001 ACE-Asia intensive observation period, *J. Geophys. Res.*, *109*, D19S02, doi:10.1029/2003JD003693.

Leaitch, W. R., et al. (2009), Evidence for Asian dust effects from aerosol plume measurements during INTEX-B 2006 near Whistler, BC, *Atmos. Chem. Phys.*, *9*, 3523–3546, doi:10.5194/acp-9-3523-2009.

Lee, C., M. Chuang, C. Chan, T. Cheng, and S. Huang (2006), Aerosol characteristics from the Taiwan aerosol supersite in the Asian yellow-dust periods of 2002, *Atmos. Environ.*, *40*, 3409–3418, doi:10.1016/j.atmosenv.2005.11.068.

Levin, Z., A. Teller, E. Ganor, and Y. Yin (2005), On the interactions of mineral dust, sea-salt particles, and clouds: A measurement and modeling study from the Mediterranean Israeli Dust Experiment campaign, *J. Geophys. Res.*, *110*, D20202, doi:10.1029/2005JD005810.

Li, J., G. Zhuang, K. Huang, Y. F. Lin, C. Xu, and S. Yu (2008), Characteristics and sources of air-borne particulate in Urumqi, China, the upstream area of Asia dust, *Atmos. Environ.*, *42*, 776–787, doi:10.1016/j.atmosenv.2007.09.062.

Ma, C., S. Tohno, and M. Kasahara (2005), A case study of the size-resolved individual particles collected at a ground-based site on the west coast of Japan during an Asian dust storm event, *Atmos. Environ.*, *39*, 739–747, doi:10.1016/j.atmosenv.2004.09.073.

Malm, W. C., J. F. Sisler, D. Huffman, R. A. Eldred, and T. A. Cahill (1994), Spatial and seasonal trends in particle concentration and optical extinction in the United States, *J. Geophys. Res.*, *99*, 1347–1370, doi:10.1029/93JD02916.

Matsumoto, K., Y. Uyama, T. Hayano, and M. Uematsu (2004), Transport and chemical transformation of anthropogenic and mineral aerosol in the marine boundary layer over the western North Pacific Ocean, *J. Geophys. Res.*, *109*, D21206, doi:10.1029/2004JD004696.

McKendry, I. G., A. M. Macdonald, W. R. Leaitch, A. van Donkelaar, Q. Zhang, T. Duck, and R. V. Martin (2008), Trans-Pacific dust events observed at Whistler, British Columbia during INTEX-B, *Atmos. Chem. Phys.*, *8*, 6297–6307, doi:10.5194/acp-8-6297-2008.

Meskhidze, N., W. L. Chameides, A. Nenes, and G. Chen (2003), Iron mobilization in mineral dust: Can anthropogenic SO_2 emissions affect ocean productivity?, *Geophys. Res. Lett.*, *30*(21), 2085, doi:10.1029/2003GL018035.

Mikami, M., et al. (2006), Aeolian dust experiment on climate impact: An overview of Japan–China joint project ADEC, *Global Planet. Change*, *52*, 142–172, doi:10.1016/j.gloplacha.2006.03.001.

Mori, I., M. Nishikawa, T. Tanimura, and H. Quan (2003), Change in the size distribution and chemical composition of kosa (Asian dust) aerosol during long-range transport, *Atmos. Environ.*, *37*, 4253–4263, doi:10.1016/S1352-2310(03)00535-1.

Nishikawa, M., S. Kanamori, N. Kanamori, and T. Mizoguchi (1991), Kosa aerosol as eolian carrier of anthropogenic material, *Sci. Total Environ.*, *107*, 13–27, doi:10.1016/0048-9697(91)90247-C.

Ooki, A., and M. Uematsu (2005), Chemical interactions between mineral dust particles and acid gases during Asian dust events, *J. Geophys. Res.*, *110*, D03201, doi:10.1029/2004JD004737.

Shen, Z. X., J. J. Cao, X. Zhang, R. Arimoto, J. Ji, W. Balsam, Y. Wang, R. Zhang, and X. Li (2006), Spectroscopic analysis of iron-oxide minerals in aerosol particles from northern China, *Sci. Total Environ.*, *367*, 899–907, doi:10.1016/j.scitotenv.2006.01.003.

Shen, Z. X., J. J. Cao, R. Arimoto, R. J. Zhang, D. M. Jie, S. X. Liu, and C. S. Zhu (2007), Chemical composition and source characterization of spring aerosol over Horqin sand land in northeastern China, *J. Geophys. Res.*, *112*, D14315, doi:10.1029/2006JD007991.

Sun, J., and T. S. Liu (2006), The age of the Taklimakan desert, *Science*, *312*, 1621, doi:10.1126/science.1124616.

Sun, J., M. Y. Zhang, and T. S. Liu (2001), Spatial and temporal characteristics of dust storms in China and its surrounding regions, 1960–1999: Relations to source area and climate, *J. Geophys. Res.*, *106*, 10,325–10,333, doi:10.1029/2000JD900665.

Sun, Y., G. Zhuang, Y. Wang, L. Han, M. Dan, J. Guo, W. Zhang, Z. Wang, and Z. Hao (2004), The air-borne particulate pollution in Beijing—Concentration, composition, distribution and sources, *Atmos. Environ.*, *38*, 5991–6004, doi:10.1016/j.atmosenv.2004.07.009.

Sun, Y., G. Zhuang, Y. Wang, X. Zhao, J. Li, Z. Wang, and Z. An (2005), Chemical composition of dust storms in Beijing and implications for the mixing of mineral aerosol with pollution aerosol on the pathway, *J. Geophys. Res.*, *110*, D24209, doi:10.1029/2005JD006054.

Sun, Y., et al. (2009), Size-resolved aerosol chemistry on Whistler Mountain, Canada with a high-resolution aerosol mass spectrometer during INTEX-B, *Atmos. Chem. Phys.*, *9*, 3095–3111, doi:10.5194/acp-9-3095-2009.

Ta, W. Q., Z. Xiao, J. J. Qu, G. S. Yang, and T. Wang (2003), Characteristics of dust particles from the desert/Gobi area of northwestern China during dust-storm periods, *Environ. Geol.*, *43*(6), 667–679.

Tang, Y., et al. (2004), Impacts of dust on regional tropospheric chemistry during the ACE-Asia experiment: A model study with observations, *J. Geophys. Res.*, *109*, D19S21, doi:10.1029/2003JD003806.

Tegen, I., and R. Miller (1998), A general circulation model study on the interannual variability of soil dust aerosol, *J. Geophys. Res.*, *103*, 25,975–25,995, doi:10.1029/98JD02345.

Wang, X. M., D. S. Xia, T. Wang, X. Xue, and J. C. Li (2008), Dust sources in and semiarid China and southern Mongolia: Impacts of geomorphological setting and surface materials, *Geomorphology*, *97*, 583–600, doi:10.1016/j.geomorph.2007.09.006.

Wang, Y., G. Zhuang, Y. Sun, and Z. An (2005a), Water-soluble part of the aerosol in the dust storm season—Evidence of the mixing between mineral and pollution aerosols, *Atmos. Environ.*, *39*, 7020–7029, doi:10.1016/j.atmosenv.2005.08.005.

Wang, Y., G. Zhuang, A. Tang, H. Yuan, Y. Sun, S. Chen, and A. Zheng (2005b), The ion chemistry and the source of PM2.5 aerosol in Beijing, *Atmos. Environ.*, *39*, 3771–3784, doi:10.1016/j.atmosenv.2005.03.013.

Wang, Y., G. Zhuang, X. Zhang, K. Huang, C. Xu, A. Tang, J. Chen, and Z. An (2006a), The ion chemistry, seasonal cycle, and sources of $PM_{2.5}$ and TSP aerosol in Shanghai, *Atmos. Environ.*, *40*, 2935–2952, doi:10.1016/j.atmosenv.2005.12.051.

Wang, Y., G. Zhuang, Y. Sun, and Z. An (2006b), The variation of characteristics and formation mechanisms of aerosols in dust, haze, and clear days in Beijing, *Atmos. Environ.*, *40*, 6579–6591, doi:10.1016/j.atmosenv.2006.05.066.

Xu, J., M. H. Bergin, R. Greenwald, J. J. Schauer, M. M. Shafer, J. L. Jaffrezo, and G. Aymoz (2004), Aerosol chemical, physical, and radiative characteristics near a desert source region of northwest China during ACE-Asia, *J. Geophys. Res.*, *109*, D19S03, doi:10.1029/2003JD004239.

Yuan, H., Y. Wang, and G. Zhuang (2003), The simultaneous determination of organic acid, MSA with inorganic anions in aerosol and rainwater by ion chromatography (in Chinese), *J. Instrum. Anal.*, *6*, 12–16.

Yuan, H., G. Zhuang, K. A. Rahn, X. Zhang, and Y. Li (2006), Composition and mixing of individual particles in dust and nondust conditions of north China, spring 2002, *J. Geophys. Res.*, *111*, D20208, doi:10.1029/2005JD006478.

Yuan, H., G. Zhuang, J. Li, Z. Wang, and J. Li (2008), Mixing of mineral with pollution aerosols in dust season in Beijing: Revealed by source apportionment study, *Atmos. Environ.*, *42*, 2141–2157, doi:10.1016/j.atmosenv.2007.11.048.

Zhang, D., and Y. Iwasaka (2004), Size change of Asian dust particles caused by sea salt interaction: Measurements in southwestern Japan, *Geophys. Res. Lett.*, *31*, L15102, doi:10.1029/2004GL020087.

Zhang, D., Y. Iwasaka, G. Shi, J. Zang, M. Hu, and C. Li (2005), Separated status of the natural dust plume and polluted air masses in an Asian dust storm event at coastal areas of China, *J. Geophys. Res.*, *110*, D06302, doi:10.1029/2004JD005305.

Zhang, R., R. Arimoto, J. An, S. Yabuki, and J. Sun (2005), Ground observations of a strong dust storm in Beijing in March 2002, *J. Geophys. Res.*, *110*, D18S06, doi:10.1029/2004JD004589.

Zhang, X., G. Zhang, Z. An, T. Chen, X. Huang, G. Zhu, and D. Zhang (1996), Element tracers for Chinese source dust (in Chinese), *Sci. China Ser. D.*, *26*(5), 421–428.

Zhang, X. Y., S. L. Gong, Z. X. Shen, F. M. Mei, X. X. Xi, L. C. Liu, Z. J. Zhou, D. Wang, Y. Q. Wang, and Y. Cheng (2003), Characterization of soil dust aerosol in China and its transport and distribution during 2001 ACE-Asia: 1. Network observations, *J. Geophys. Res.*, *108*(D9), 4261, doi:10.1029/2002JD002632.

Zhao, X., G. Zhuang, Z. Wang, Y. Sun, Y. Wang, and H. Yuan (2007a), Variation of sources and mixing mechanism of mineral dust with pollution aerosol—Revealed by the two peaks of a super dust storm in Beijing, *Atmos. Res.*, *84*, 265–279, doi:10.1016/j.atmosres.2006.08.005.

Zhao, X., Z. Wang, G. Zhuang, and C. Pang (2007b), Model study on the transport and mixing of dust aerosols and pollutants during an Asian dust storm in March 2002, *Terr. Atmos. Oceanic Sci.*, *18*(3), 437–457, doi:10.3319/TAO.2007.18.3.437(EA).

Zhuang, G., Z. Yi, R. A. Duce, and P. R. Brown (1992), Link between iron and sulfur suggested by the detection of Fe(II) in remote marine aerosols, *Nature*, *355*, 537–539, doi:10.1038/355537a0.

Zhuang, G., J. Guo, H. Yuan, and C. Zhao (2001), The compositions, sources, and size distribution of the dust storm from China in spring of 2000 and its impact on the global environment, *Chin. Sci. Bull.*, *46*(11), 895–900, doi:10.1007/BF02900460.

J. S. Fu, Department of Civil and Environmental Engineering, University of Tennessee, Knoxville, TN 37996, USA.

K. Huang, J. Li, Y. Lin, Q. Wang, and G. Zhuang, Center for Atmospheric Chemistry Study, Department of Environmental Science and Engineering, Fudan University, Shanghai 200433, China. (gzhuang@fudan.edu.cn)

Y. Sun, Atmospheric Sciences Research Center, State University of New York at Albany, Albany, NY 12203, USA.